Hydrogen Bond Dynamics of Histamine Monocation in Aqueous Solution: Car−Parrinello Molecular Dynamics and Vibrational Spectroscopy Study

ARTICLE *in* THE JOURNAL OF PHYSICAL CHEMISTRY B · MAY 2011

Impact Factor: 3.3 · DOI: 10.1021/jp111175e · Source: PubMed

6 AUTHORS, INCLUDING:

Jernej Stare
National Institute of Chemistry
41 PUBLICATIONS **427** CITATIONS
SEE PROFILE

Janez Mavri
National Institute of Chemistry
99 PUBLICATIONS **1,680** CITATIONS
SEE PROFILE

Joze Grdadolnik
National Institute of Chemistry
56 PUBLICATIONS **1,263** CITATIONS
SEE PROFILE

Robert Vianello
Ruđer Bošković Institute
64 PUBLICATIONS **883** CITATIONS
SEE PROFILE

THE JOURNAL OF PHYSICAL CHEMISTRY B

ARTICLE

pubs.acs.org/JPCB

Hydrogen Bond Dynamics of Histamine Monocation in Aqueous Solution: Car−Parrinello Molecular Dynamics and Vibrational Spectroscopy Study

Jernej Stare,[†] Janez Mavri,[†,‡] Jože Grdadolnik,[†,‡] Jernej Zidar,[†,‡] Zvonimir B. Maksić,[∥,§] and Robert Vianello*[,†,§]

[†]National Institute of Chemistry, Hajdrihova 19, SI-1000 Ljubljana, Slovenia

[‡]EN→FIST Centre of Excellence, Dunajska 156, SI-1000 Ljubljana, Slovenia

[§]Ruđer Bošković Institute, Bijenička cesta 54, HR-10000 Zagreb, Croatia

Supporting Information

ABSTRACT: Hydration of histamine was examined by infrared spectroscopy and Car−Parrinello molecular dynamics simulation. Histamine is a neurotransmitter and inflammation mediator, which at physiological pH conditions is present mainly in monocationic form. Our focus was on the part of vibrational spectra that corresponds to histamine N−H stretching, since these degrees of freedom are essential for its interactions with either water molecules or transporters and receptors. Assignment of the experimental spectra revealed a broad feature between 3350 and 2300 cm^{-1}, being centered at 2950 cm^{-1}, which includes a mixed contribution from the ring N−H and the aminoethyl N−H stretching vibrations. Computational analysis was performed in two ways: first, by making Fourier transformation on the autocorrelation function of all four N−H bond distances recorded during CPMD run, and second, and most importantly, by incorporating quantum effects through applying an *a posteriori* quantization of all N−H stretching motions utilizing our snapshot analysis of the fluctuating proton potential. The one-dimensional vibrational Schrödinger equation was solved numerically for each snapshot, and the N−H stretching envelopes were calculated as a superposition of the 0→1 transitions. The agreement with the experiment was much better in the case of the second approach. Our calculations clearly demonstrated that the ring amino group absorbs at higher frequencies than the remaining three amino N−H protons of the protonated aminoethyl group, implying that the chemical bonding in the former group is stronger than in the three amino N−H bonds, thus forming weaker hydrogen bonding with the surrounding solvent molecules. In this way the results of the simulation complemented the experimental spectrum that cannot distinguish between the two sets of protons. The effects of deuteration were also considered. The resulting N−D absorption is narrower and red-shifted. The presented methodology is of general applicability to strongly correlated systems, and it is particularly tuned to provide computational support to vibrational spectroscopy. Perspectives are given for its future applications in computational studies of tunneling in enzyme reactive centers and for receptor activation.

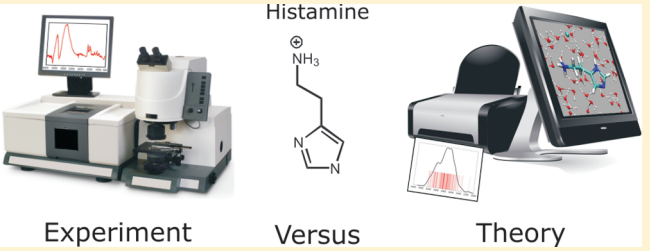

INTRODUCTION

Infrared (IR) and Raman spectroscopic investigations of the hydrogen bond dynamics continue to trigger considerable theoretical and experimental interest and efforts, as these methods are among the most powerful techniques for characterizing medium−size molecules in condensed phases. This is a consequence of the fact that hydrogen bonding and the subsequent proton transfer reactions encompass the most fundamental (bio)chemical transformations, being also of the outmost importance for a variety of phenomena in chemistry, biology, and industry.[1−4] For example, protonation and deprotonation of the starting substances are the initial steps of many chemical synthetic pathways.[5,6] Further, tautomeric proton transfer in hydrogen bonded base pairs of DNA and proton relay systems in many enzymes are typical examples of biological reactions.[4,7] Finally, hydrogen bonding has recently been revitalized as a crucial type of interaction in receptor activation,[8] trans-membrane transport[9] and ion-channels gating.[10−12]

One of the important small molecules playing significant roles in both molecular biology and molecular medicine is histamine. Since its first pharmacological description as an endogenous substance in 1910,[13] histamine has proven to be an important biogenic amine.[14,15] It participates in complex biological processes related to intercellular communication, defense, and cell proliferation in mammals.[16] In recent years, it has gained importance as a neurotransmitter in processes of sleep−wake cycles,

Received: November 23, 2010
Revised: April 7, 2011
Published: April 25, 2011

appetite control, learning, memory, and emotion.[17,18] Moreover, its signaling pathways seem to be involved in conditions such as depression, schizophrenia, Alzheimer's disease, and epilepsy.[18] Consequently, processes involving histamine transport, metabolism, and binding to macromolecules through hydrogen bonding have a significant physiological relevance. It is the purpose of this work to shed more light on the structure, hydrogen bonding ability, and hydration dynamics of histamine in aqueous solution by Fourier transform infrared (FTIR) spectroscopic and computational chemistry methods.

Although we are witnessing continuous progress in the experimental spectroscopy setups, a proper assignment of the vibrational spectra of hydrogen−bonded systems is far from being straightforward. One of the characteristic features of the IR spectra of such a system is a complicated band shape of the stretching vibration band of the X−H group engaged in the hydrogen bond interaction.[19] In medium strength and in strongly hydrogen-bonded systems in particular, the ν(X−H) band is relatively broad, intense, and exhibits complex structure.[20] However, in past years new developments in experimental nonlinear techniques[21] have allowed the direct examination not only of vibrational frequencies, but also of the specific anharmonicities of vibrational modes.[22] This additional information demands a more quantitative interpretation of the different contributions determining the overall vibrational spectrum. It is gratifying that rapid development in computer hardware and quantum chemistry software allowed for very accurate estimates of low-lying vibrational levels of semi-rigid polyatomic molecules in the gas-phase employing quantum-mechanical methodologies.[23,24] These methodologies, however, are either highly cost−effective or not feasible for larger systems, if good accuracy is desired. Recently, application of anharmonic force fields[25−27] or the additivity of anharmonic corrections[28] in conjunction with the density functional theory (DFT) has led to improved agreement with the experimental data. On the other hand, *ab initio* frequency calculations are in most cases restricted to harmonic approximation without thermal averaging. Vibrational self-consistent field (VSCF),[29] though, is capable of treating moderately anharmonic systems, but it is of limited use in the systems exhibiting strong anharmonicity and possessing multiple minima. Another important point is that the gas-phase results yield important inherent properties of investigated molecules relieved of any solvent or counterion influence. This will be examined too. However, it is necessary to include a realistic fluctuating environment into simulations, because most of the experimental determinations are performed in the condensed phase. This holds for both the biologically and industrially interesting processes. Consequently, we felt it worthwhile to include in the computational treatment of histamine both anharmonicity and specific solute−solvent interactions. The dynamical behavior of the studied molecule was examined by DFT-based Car−Parrinello molecular dynamics (CPMD),[30] conducted at the experimental temperature, and performing an *a posteriori* quantization of the particular nuclear motions.[31] This is a necessity, because the proton motion in hydrogen bonds is essentially quantum in its nature,[32,33] which makes the computational treatment of the hydrogen bonded systems very demanding, since solutions of the vibrational Schrödinger equation are required. On the other hand, molecular dynamics (MD) procedures are essential methods of choice for including temperature and conformational dynamics in the computations with a distinct advantage that entropic effects are directly taken into account. For the sake of completeness, we mention that there is a number of other computational strategies in the literature aimed at resolving these difficulties.[34−44] However, we would like to present the potential and the accuracy of the computational methodology, involving quantization of the nuclear motion on snapshot structures extracted from the explicit solvent CPMD simulation, as an illustration of the condensed phase computational spectroscopy.

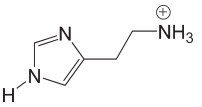

Figure 1. The investigated histamine monocation.

The structure of a histamine molecule in water is the result of a multiple Brønsted acid−base equilibrium. The neutral free−base histamine is composed of an imidazole ring and an aminoethyl side-chain (Figure 1), both of which have the ability of accepting a proton, if the medium is acidic enough. At physiological pH of 7.4, only the free amino group is protonated, as deduced from the two pK_a values of histamine. They assume values of 5.8 (imidazole ring nitrogen atom) and 9.4 (aliphatic primary amine nitrogen atom).[45,46] Hence, histamine is largely a monocation (96%). Previous computational studies on histamine in aqueous solutions have been mostly concentrated on structural (conformational and tautomeric)[47,48] and vibrational properties[49] of this compound using a simple implicit solvation picture through the polarized continuum model (PCM) or on calculations of its pK_a acidity constants using the Langevin dipoles solvation model.[46] It is, therefore, of interest to provide results obtained on a more sophisticated level and relate them to earlier ones.

Spectroscopic characterization of neutral histamine in water was accomplished for the first time recently by Ramírez and co-workers using FTIR and Raman spectroscopy.[47] The spectra revealed similarities in the position and shapes of absorption bands compared to monocation spectra obtained by the same group earlier.[49] The first such study of the histamine monocation was performed by Bellocq and Garrigou-Lagrange as early as 1970.[50] Ramírez and co-workers recorded IR and Raman spectra of the protonated histamine in water and D_2O, supplemented by a static dielectric continuum model B3PW91/6-31+G(d) calculations.[49] Unfortunately, the authors did not present any experimental or computational results in the part of the spectra above 1600 cm^{-1} in H_2O, which largely corresponds to the N−H stretching vibrations. The latter represent vibrational degrees of freedom, which are essential for histamine's specific interactions with the environment, consequently being very important for its biological activity and function. Also, these vibrations are affected the most by the presence of water molecules. Investigations of these N−H stretching vibrations are complicated and pose a big challenge for the computational treatment of aqueous histamine, because of the anharmonic potentials involved and the necessity for quantization of the N−H stretching motion due to low mass of the proton as pointed out above.

As a final note, it is worth mentioning that histamine has been studied in the solid state,[51,52] and as a complexation agent for several transition metals.[53−55] Related theoretical and experimental work on the physiologically relevant histamine monocation,[49−59] revealed that the trans conformer N^{τ}−H is the predominant structure (80%) in solution (Figure 1). Hence, the structure of the histamine monocation in the N^{τ}−H trans conformation and its deuterated counterpart histamine^{+}−Nd_4 are the primary focus of the present investigations.

EXPERIMENTAL SECTION

Histamine free base (>97%, Sigma) was used without further purification. 1 M solution of histamine in H_2O was prepared by dissolving the appropriate amount of dry histamine in mQ water. The corresponding D_2O solution was, in order to achieve better deuteration, prepared from the histamine, which was previously twice dissolved in D_2O and dried in nitrogen atmosphere. By comparing the intensity of D_2O and HDO stretching peaks, it turned out that the extent of deuteration was over 90%. The pH was adjusted at 7.4 by adding appropriate amounts of HCl (DCl). IR spectra were taken on a Perkin-Elmer System 2000 IR spectrometer equipped with Golden Gate temperature stabilized diamond attenuated total reflectance (ATR) cell. All spectra were recorded at 25 °C. Typically 256 interferograms were averaged and apodized with Happ−Genzel function. To avoid distortions due to anomalous dispersion, the original ATR spectra were recalculated to obtain a pure absorption spectrum using the method originally described by Bertie and Lan.[60] The method is upgraded by application of calibration procedure, which minimizes the distortions of the imperfect optical path in the ATR cell.[61,62] The calibration of the optical path was done by recording the spectra of pure water.

COMPUTATIONAL DETAILS

We performed CPMD[30] simulations of histamine monocation immersed in liquid water (H_2O), where the positions of the atoms evolve according to the classical Newton equations of motion, on the basis of forces obtained directly from the instantaneous electronic structure calculated within the DFT formalism. As the starting geometry for our system, we used the one obtained by BLYP energy minimizations in vacuum. The system was electrically neutralized with one chloride (Cl^-) anion, which allowed the three-dimensional periodicity of the system to be fully considered. The chloride anion was placed in a box close to the charged $-NH_3^+$ group with imposed nitrogen−chlorine harmonic restraint for the equilibrium distance of 5.0 Å and the force constant of 6.27 kcal mol^{-1} A^{-2}. As such, during simulation, the chloride anion would not come close to the protonated amino group and influence its dynamics. The selection of restrain parameters is somewhat arbitrary, but it is well justified from the insight offered by the classical force-field MD (see later). The solute was soaked by using an equilibrated water box. We selected a cubic box of water molecules with the cell dimension of a = 14.4594 Å. This allowed for 93 water molecules in total, optimized in a way that such pure water had a density of 1 g cm^{-3}. The size of the box and the corresponding number of water molecules enabled histamine to be surrounded by a solvation shell sufficiently large to adopt all of the often specific structures relevant to the aqueous chemistry of this solute. Periodic boundary conditions were employed with the Ewald summation technique to calculate the electrostatic interactions. All CPMD simulations were performed with the CPMD program package version 3.13.2.[63] The CPMD calculations employ the BLYP functional[64] with Trouillier−Martins[65] atomic pseudopotentials for core electrons. Hydrogen atoms were represented by a simple s potential with a 0.5 au radius damping the Coulomb singularity at the origin. The kinetic energy cutoff for the plane-wave basis set was set to 70 Ry. This cutoff value was selected after a series of periodic single-point calculations on a random geometry, changing cutoff value from 50 to 200 Ry and monitoring convergence behavior of the energy and forces as a function of the cutoff value. The cutoff value of 70 Ry was selected as the best compromise between the accuracy and the feasibility of the simulation. Details on these benchmark calculations are given in the Supporting Information. A Γ-point approximation was used, because the simulation cell was reasonably large. The solvent−solute system was first equilibrated for 1 ps with initial velocities obtained from a 300 K Maxwell distribution. Data were then collected through productive dynamics over 10 ps. This time window is just long enough to observe a number of important dynamical processes characteristic for liquid water, in particular hydrogen-bond breaking and rearrangement (around 2−3 ps). The average temperature was 300 K during our simulation, which was controlled by the Nosé−Hoover chain thermostat[66−68] with the coupling frequency of 1500 cm^{-1}. We used a fictitious orbital mass of 500 atomic units and the MD integration time step of 4 au (0.09675 fs). It turned out that during the overall CPMD run there appears to be a drift of about 0.02 au in the electron kinetic energy. This is potentially dangerous, because it means that the electrons are uncontrollably moving away from the Born−Oppenheimer surface. We consider this drift to be small enough not to interfere too severely with the MD. This drift is, however, compensated by a decrease of the total classical energy. Therefore, it is important to mention that the observed total Hamiltonian energy appears not to be drifting. Its drift is around 2.5×10^{-4} a.u. during the whole 10 ps of the CPMD simulation, which means that it assumes a value of 8.3×10^{-8} a.u. ps^{-1} $atom^{-1}$. As such, it is more than an order of magnitude below the threshold in the total Hamiltonian energy drift of 10^{-6} a.u. ps^{-1} $atom^{-1}$, as recommended by VandeVondele and co-workers.[69]

The resulting computational IR spectra of the N−H stretching modes were subsequently obtained by using two independent approaches. First, the time autocorrelation function of selected bond distances was extracted from the CPMD trajectory, from which the IR absorption spectrum was obtained through Fourier transformation. Second, we applied an *a posteriori* quantization of all N−H stretching motions utilizing snapshot analysis of the fluctuating proton potential. A number of preceding studies have also addressed the idea of snapshots in which the vibrational Shrödinger equation was solved for vibrational chromophores in a frozen environment.[31,70−74] Our previous experience in this field involved implementation of the snapshot envelope method within the CPMD simulations to much shorter and stronger hydrogen bonds with the characteristic effects in the crystalline environment of an inorganic compound.[31] The present study is a complementary critical validation of this methodology in a system of considerably different characteristics, since histamine is a biological molecule exhibiting medium−strong hydrogen-bonding interactions being immersed in liquid water.

Snapshot structures of the CPMD trajectory were extracted every 2500 steps, which corresponds to a time step of about 237 fs. Such an interval was chosen to minimize correlation between snapshots while providing a sufficient number of structures. In such a way, 42 distinct structures were obtained. Four one-dimensional proton potential functions along the N−H lines were constructed from each of these structures, making use of single-point CPMD periodic calculations, by displacing one of the four N−H hydrogen atoms in histamine from r(N−H) = 0.8 Å to r(N−H) = 2.0 Å with 0.1 Å resolution, i.e., steps. In doing so, all other nuclei were kept frozen in their instantaneous positions, as extracted from the trajectory, thus corresponding to a single point potential energy scan. Four typical proton potentials obtained from snapshot structures are graphically depicted in Figure 2.

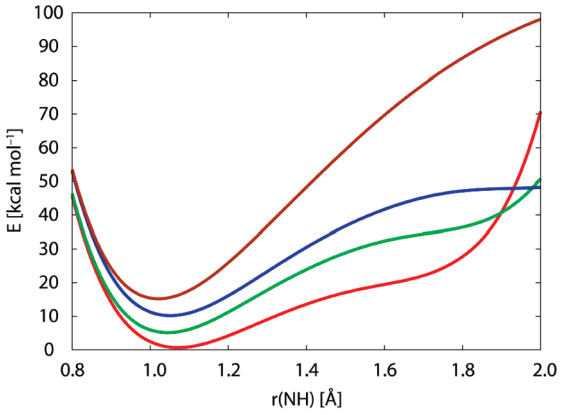

Figure 2. Sample proton potentials, extracted from snapshots after the CPMD simulation.

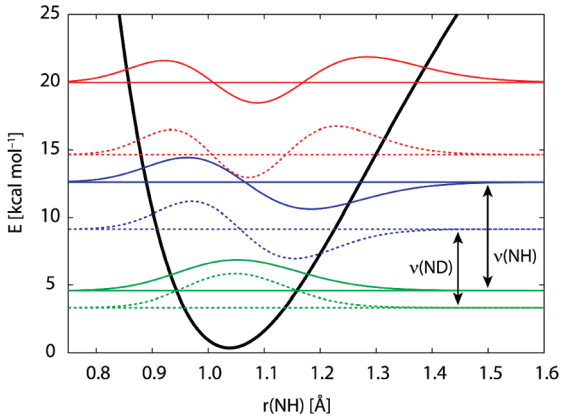

Figure 3. Three lowest vibrational levels and the corresponding wave functions for N−H (full lines) and N−D (dashed lines) stretching vibrations obtained by solving the vibrational Schrödinger equation on a sample potential (black line). The fundamental 0→1 transitions for H and D are also indicated by doubly tipped arrows.

A total number of 126 primary aliphatic amino and 42 tertiary ring amino proton potentials were obtained in this way. Although this is likely to be a rough approximation of the actual proton motion, an underlying tacit assumption is that all N−H stretching motions are much faster than the other vibrational degrees of freedom, implying that all four hydrogen atoms represent four independent quantum particles and not a coupled many-body quantum problem. Having the potential energy function at hand, the vibrational analysis for each snapshot of the each N−H motion has been carried out by solving the one-dimensional vibrational Schrödinger equation using the variational Fourier Grid Hamiltonian method[75] tuned for the application in generalized internal coordinates.[37] The resulting discrete vibrational levels together with their corresponding wave functions and energies give rise to the N−H stretching frequencies beyond the harmonic approximation. Since the reduced mass for the motion along the stretching coordinate is required as input, this approach allows for the consideration of isotope effects applying a different mass corresponding to the isotope change. Therefore, we performed the calculations of vibrational levels for both undeuterated and deuterated species of the title compound. A sample potential with corresponding vibrational energy levels and wave functions is shown in Figure 3.

When calculating the vibrational spectra, we considered only 0→1 transitions for each proton potential. The contribution of the NH (ND) stretching band to the vibrational spectrum [also called the NH (ND) stretching envelope] was obtained as a set of lines, each line corresponding to the 0→1 transition calculated from its snapshot potential. The distribution of the resulting vibrational transitions was plotted against the frequency axis as a set of delta functions. In addition, the envelope was approximated by a continuous curve, arbitrarily assuming that each individual vibrational transition is a Gaussian function of a constant half-width of 50 cm^{-1}. The presented methodology is also applicable for studies of nuclear quantum effects in biological systems in the context of the quantum-mechanics/molecular-mechanics (QM/MM) approach.

In order to check the conformational flexibility of histamine in aqueous solution, we also performed a classical force-field MD simulation involving ethylamino-protonated histamine and a total of 735 water molecules immersed in a cubic simulation box with the edge of 27 Å. The chloride anion Cl^- was again added to the box to ensure the overall electroneutrality. A standard CHARMM force field[76] was applied for protonated histamine and the chloride ion, and the TIP3P water model was utilized for solvent molecules as implemented within the CHARMM program package.[77] Long-range electrostatics was treated with the particle mesh Ewald summation technique.[78] MD simulation was performed at a constant temperature of 300 K and a constant pressure of 1 bar using a Nosé−Hoover thermostat.[68] The following non-bonding cutoff values were used: CUTNB = 4.0 Å, CTOFNB = 0.0 Å, and CTONNB = 7.0 Å. The simulation was performed for 7 ns, applying an integration step of 1 fs, which is sufficient to observe conformational changes, and where the first nanosecond of the simulation was used for the equilibration. Trajectory was stored every 100 fs. The analysis of the obtained classical trajectory was carried out using the VMD program.[79]

Examination of the intrinsic microsolvation effects and the vibrational features of protonated histamine were performed in the gas-phase using the Gaussian 09 suite of programs.[80] All molecular geometries were optimized and thermodynamic parameters calculated by the B3LYP/6-311+G(d,p) method. Analysis of all normal vibrational modes at the same level of theory was used to verify that all structures correspond to true minima on the electronic Born−Oppenheimer potential energy surface. The microsolvation effects on protonated histamine were evaluated through interaction energies of histamine monocation with a single water molecule specifically placed to form an optimal hydrogen bonding interaction with particular acidic/basic site on the histamine. The energies of these interactions were attained through single-point calculations performed using a highly flexible and very large basis-set within the B3LYP/6-311++G(3df,3pd) scheme. The implicit solvation was included through the PCM[81] utilizing default parameters for water, giving rise to the (PCM)/B3LYP/6-311++G(3df,3pd)//(PCM)/B3LYP/6-311+G(d,p) methodology. All interaction energies were calculated as enthalpies of reaction subtracting the total molecular enthalpies of individual histamine and water molecules from the enthalpy of a formed 1:1 complex.

RESULTS AND DISCUSSION

Experimental Vibrational Spectra. The application of ATR spectroscopy enables the study of the high frequency region

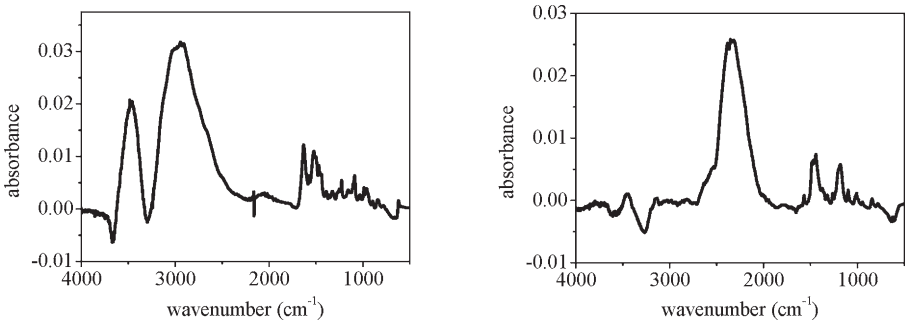

Figure 4. The processed absorbance spectrum of 1 M histamine in monocation form recorded in H_2O (left) and in D_2O (right). The spectrum of bulk water is subtracted.

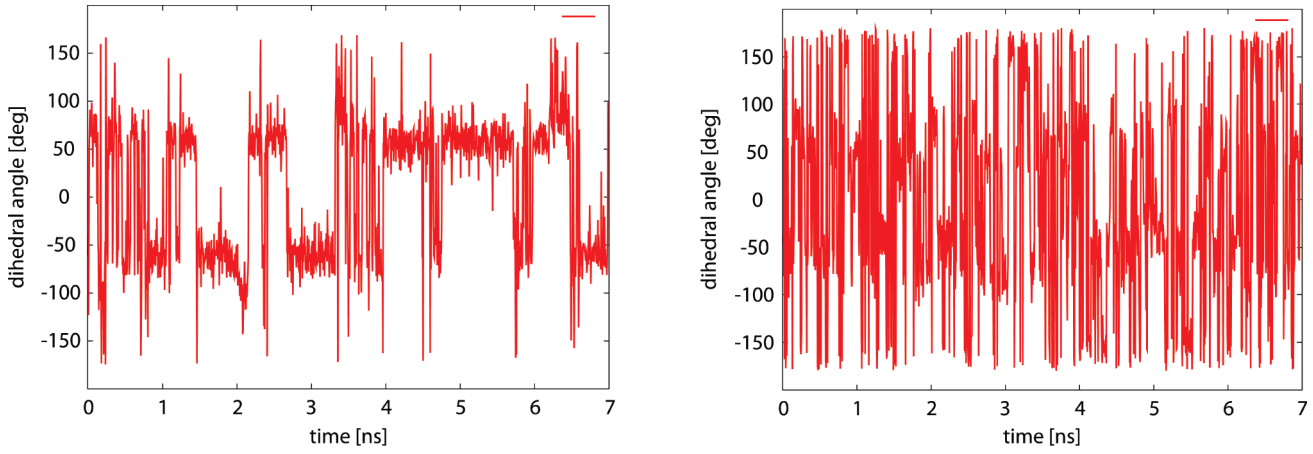

Figure 5. Changes in the dihedral angle for the rotation of the five-membered ring (left) and the protonated amino group (right) around single C−C and N−C bonds, respectively, during classical MD simulation.

characteristic for H_2O and NH stretching vibrations. Moreover, the modest intensity of these bands ensures the accurate subtraction of a spectrum of bulk water. The processed absorption spectra of 1 M histamine in monocation form (pH = 7.4) in H_2O and in D_2O are presented in Figure 4. For an interested reader, raw spectra without processing are presented in the Supporting Information. The spectrum of bulk H_2O or D_2O was subtracted in both cases. The assignment of the bands of histamine followed the assignment of Collado and co-workers.[49] The region between 3600 cm^{-1} and 2300 cm^{-1} in the spectrum of histamine in H_2O is characteristic for the stretching vibrations of H_2O and NH groups. Subtraction of bulk water significantly reduces the intensity of OH stretching, which is dominant in the solution spectrum. After subtraction, two broad features remain in the high frequency region. One is centered at 3485 cm^{-1} and belongs to the residual of the main H_2O stretching band. The more intense one is the broad band centered at 2950 cm^{-1}. The full width at half-intensity (FWHI) of this band is 450 cm^{-1}. The shape of the band indicates the complex intrinsic band structure. We assigned this band to the NH stretching modes. This band should include three different modes of NH stretching of histamine, i.e., stretching of the imidazole NH group and symmetric and antisymmetric stretching of the $-NH_3^+$ group, respectively. In general, the imidazole NH stretching should appear at higher wave numbers with respect to the antisymmetric and symmetric $-NH_3^+$ vibrations, but that is difficult to distinguish using only spectroscopic methods. The corresponding band in the spectrum of D_2O solution is centered at 2340 cm^{-1} and belongs to the stretching vibration of ND atoms within the imidazole ring and $-ND_3^+$ antisymmetric and symmetric stretching band. The entire band is narrower with FWHI equal to 270 cm^{-1}. The remaining OD stretching band after subtraction is represented as a shoulder near 2520 cm^{-1}.

Computational Analysis. The first piece of information that can be obtained from an MD trajectory of 10.0 ps length is a fairly accurate description of the geometric and dynamical properties of the solvent surrounding the histamine molecule and the effect on the solute geometry. During CPMD simulation, we observed no major conformational change in the histamine, meaning that the trans conformation of the aminoethyl side-chain was preserved, and that we detected no rotation of the five-membered ring around the single C−C bond. The CPMD simulated time of about 10 ps is obviously not long enough to observe internal histamine rotations giving rise to gross conformational changes. Moreover, a relatively small simulation box may have serious impact on the electrostatics. Therefore, we performed a much longer 7 ns classical MD simulation taking into account a large number of water molecules. During that simulation, we recorded the changes in two relevant dihedral angles crucial for the conformational freedom of this molecule and the resulting vibrational spectra. The first dihedral angle defines rotation of the five-membered ring around the single C−C bond, whereas the second one describes the rotation of the free amino group around the single N−C bond. The results are depicted in Figure 5.

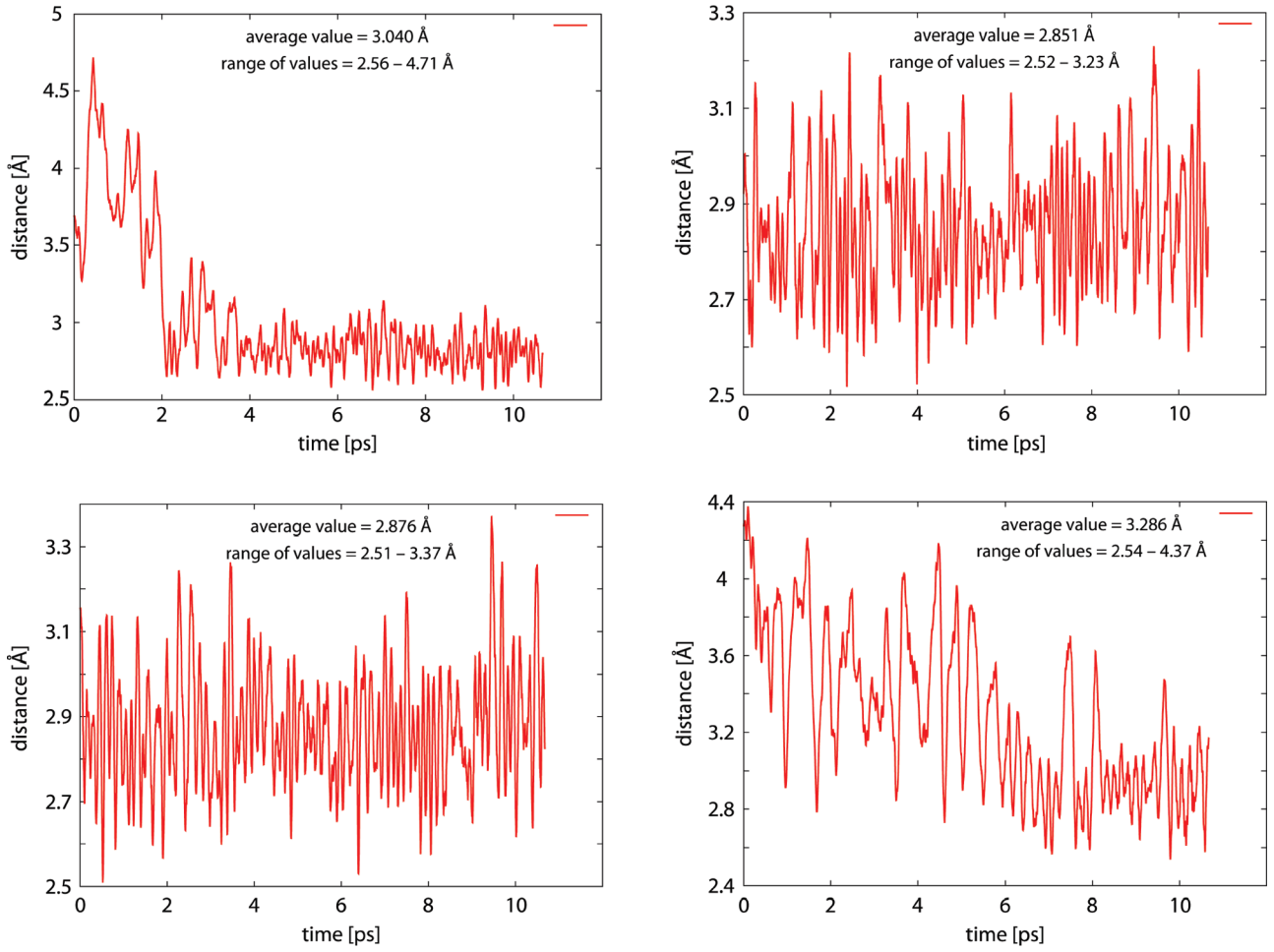

Figure 6. Evolution of the three N···O(water) bond distances from the protonated free-amino group (top row and bottom left) and of the H(histamine)—O(water) bond distance from the ring amino group (bottom right) during CPMD simulation.

The results in Figure 5 reveal that the five-membered ring is not as flexible as it could be assumed. During simulation, the corresponding dihedral angles cluster mostly around the values of +60° and −60°, meaning that the conformational flexibility of this ring is restricted only to a third of a full cycle. Therefore, it can be safely concluded that the histamine conformation adopted in our CPMD simulation represents an important population of the classical simulation, which is additional proof of the validity of the CPMD spectra simulation. Also, these changes in the classical simulation (Figure 5) occur on a nanosecond time scale, which is at the moment well beyond the CPMD simulation time. The situation with the protonated free-amino group is more complicated. The plot on the right-hand side of the Figure 5 reveals that this group can freely make full-cycle rotation. However, it is important for the calculation of the vibrational spectra to notice that during CPMD simulation there was practically no exchange of the solvent water molecules around vibrating N—H atoms. To validate this conjecture, we extracted all four amino N···O-(water) bonds distances from the CPMD trajectory (Figure 6) as well as radial distribution functions $g(r)$ around all three amino nitrogen atoms from the classical simulation (Figure 7).

The broad picture of the hydration of histamine emerging from the simulation conforms to what could be anticipated for this class of aqueous molecules. The free—amino group and both ring nitrogen atoms participate fully in solute—water intermolecular hydrogen bonding. The average number of solvent molecules hydrogen bonded to the main hydrophilic sites of histamine is therefore five. It is interesting to observe that, although the $-NH_3^+$ group is conformationally very flexible and it is free to rotate around the N—C bond during simulation, each of the three amino protons is always preferentially bound to the same water molecule in the resulting trajectory. In other words, there is practically no exchange between water molecules to compete for the hydrogen bonding with this charged group, at least on the time scale of the present CPMD simulation. Specifically, all three corresponding N···O distances of the free-amino group take on average values of 3.040, 2.851, and 2.876 Å (Figure 6). The first value is a bit larger than the remaining two simply because during the first two picoseconds of the equilibration dynamics this bond length assumes high values, well above 3.3 Å (Figure 6). However, for the remaining 8 ps of the simulation the average value of this N···O distance is 2.852 Å, which makes it equivalent to the remaining two N···O values within this group.

The same observation holds in the case of the amino N—H bond in the five—membered ring. It is bound to the oxygen atom of the closest water molecule, with the O···N distances within the range of 2.54—4.37 Å, taking on an average of 3.286 Å. These values are very indicative of the strength of the interaction between these two hydrophilic sites in histamine and the surrounding water molecules. Simply taking into account the

dx.doi.org/10.1021/jp111175e |J. Phys. Chem. B 2011, 115, 5999–6010

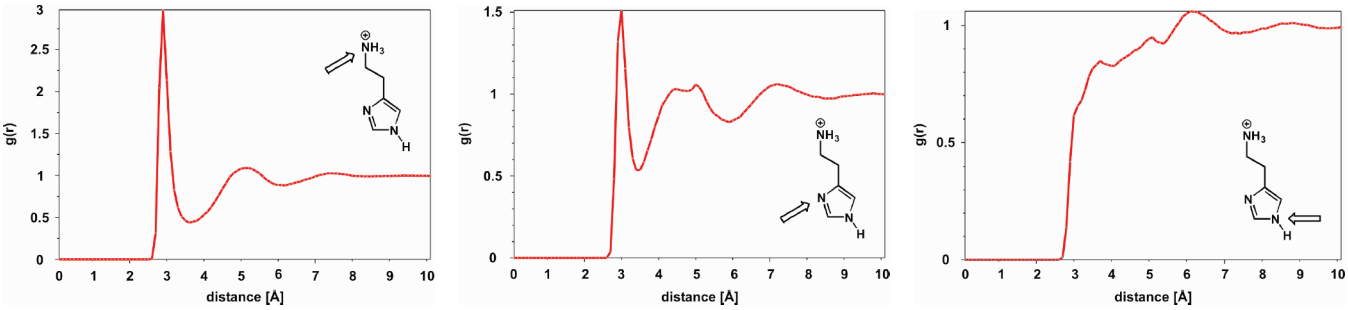

Figure 7. Radial distribution function $g(r)$ of N(histamine)···O(water) distances for all three nitrogen atoms in the protonated histamine as calculated from the classical MD simulation.

above-mentioned average bond distances, one concludes that the ring amino group has considerably weaker interaction with the solvent molecules, since its average N···O distance is larger. This conjecture is also evidenced through the inspection of the relevant radial distribution functions calculated between all three histamine nitrogen atoms and water oxygen atoms, presented in Figure 7. This plot for the chain-amino nitrogen atom reveals a higher first hydration peak compared to that of the corresponding ring nitrogen amino atom. This is additional evidence that the protonated free-amino group forms stronger hydrogen bonds with water molecules than the corresponding ring nitrogen atoms.

In order to validate this conclusion even further, we performed static DFT analysis coupled with the PCM implicit water solvation approach. It turned out that the (PCM)/B3LYP/6-311++G(3df,3pd)//(PCM)/B3LYP/6-311+G(d,p) calculations gave enthalpies of interaction between histamine monocation and a single water molecule of −5.1, −4.9, and −4.8 kcal mol^{-1} in the case of the three amino protons in the $-NH_3^+$ group, whereas it was just −2.3 kcal mol^{-1} for the ring amino group. It is worth noting that each H_2O molecule was specifically bound to its N−H proton counterpart in a way to form an optimal hydrogen bonding interaction. It should be strongly emphasized that the observed hierarchy and differences in the strength of the interaction between two N−H sites in histamine and the neighboring water solvent molecules are in harmony with the observed N−H stretching frequencies, as it will become apparent later in the text.

As a final note, it should be reiterated that during CPMD simulation the distance between the chlorine anion and the nitrogen of the charged $-NH_3^+$ group was harmonically restrained to the distance of 5.0 Å, and that it oscillated between 4.65 and 5.37 Å. In contrast to CPMD, in classical MD we did not impose any geometrical restraints on the chloride anion. The ion freely moved in the unit cell, and because of the much larger size of the simulation cell it came to the vicinity of the histamine very rarely. Therefore, the applied restraints in the CPMD run are well justified. It should be also emphasized that the CPMD simulation time was not long enough to observe any proton transfer, either from the histamine N−H groups to water molecules or from water molecules to the basic sites on histamine, particularly to the imino nitrogen within the five-membered ring. This is consistent with the calculated proton potentials (Figure 2), which reveal no tendency of the proton transfer or the second minimum.

Vibrational Spectra from the Autocorrelation Function of Bond Distances. One of the main difficulties in working with vibrational spectroscopy in aqueous solution originates from the fact that water molecules exhibit a very intense IR activity, which makes the signal of the hydrated solute usually completely obscured. This is a problem both in experiment and in computations. It has been demonstrated in numerous occasions that *ab initio* MD simulation, combined with time correlation function methods, is a useful tool for computational modeling and interpretation of the condensed−phase vibrational spectra. The pioneering study in the field was a first-principle calculation of the IR absorption of liquid water[82] and ice at high pressure[83] by Silvestrelli, Bernasconi, and Parrinello, followed by the computation of the Raman spectrum of ice by Putrino and Parrinello[84] using density functional perturbation methods. Similar to most of the classical mechanics computational investigations performed nowadays, the resulting spectrum in the aforementioned studies[82−84] was obtained by Fourier transformation of the time correlation function of the total dipole moment of the system, since the latter was not influenced by any kind of solvent molecules.

One of the ways to isolate just the IR signal of aqueous solutes is to consider the time correlation function of the selected bond distances relevant for the stretching vibrations. The underlying assumption is that the dipole moment function $\mu(x)$ is linear with respect to bond distance x (the electronic contribution to the dipole moment was assumed to be harmonic, i.e., electric harmonicity). We verified this assumption by stepwise changing the N−H bond distance in either the ring or chain-amino group from 0.95 to 1.10 Å (which roughly corresponds to the N−H bond oscillation amplitude during CPMD simulation at the specified conditions), and by performing a single point calculation followed by the Wannier function localization at each step.[85] This procedure yields the location of Wannier centers, which represent the position of electron pairs for each N−H distance. Since for both the ring and the chain-amino groups the corresponding Wannier centers of the N−H bonds lie on the N−H bond lines in most cases, one can use the correlation plot of the distance between nitrogen and the Wannier center against the N−H bond distance as a reasonable measure for the electronic harmonicity of the local dipole of the N−H bond. The plot is displayed in Figure 8.

It can be clearly seen that for both the ring and the chain-amino groups, the location of the Wannier center of the N−H bond varies practically linearly with the N−H bond distance. Thus, the local dipole vector of the N−H bond can be safely regarded as a linear function of the N−H bond distance, and the approximation of the harmonicity of the local electron density center is justified. Note, though, that the slopes of the dipole moment function are not equal for ring and free amino groups (the former being by about 10% steeper than the latter), suggesting that the contribution of the ring amino group to the IR spectrum is by about 10% larger than that of the free amino

dx.doi.org/10.1021/jp111175e |*J. Phys. Chem. B* 2011, 115, 5999–6010

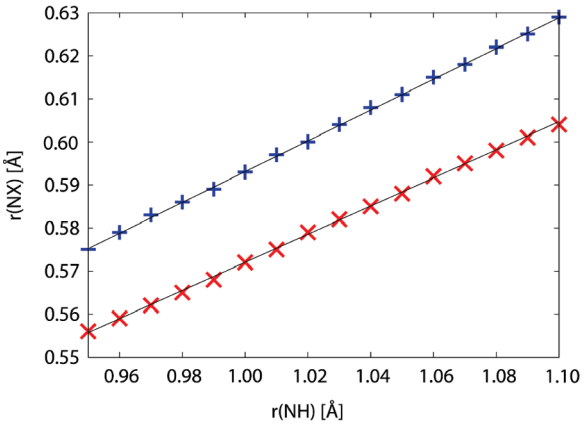

Figure 8. Distance between nitrogen and the Wannier center of the N−H bond [r(NX)] as a function of the N−H distance. Blue points correspond to the ring NH group, while red points represent a free amino NH group.

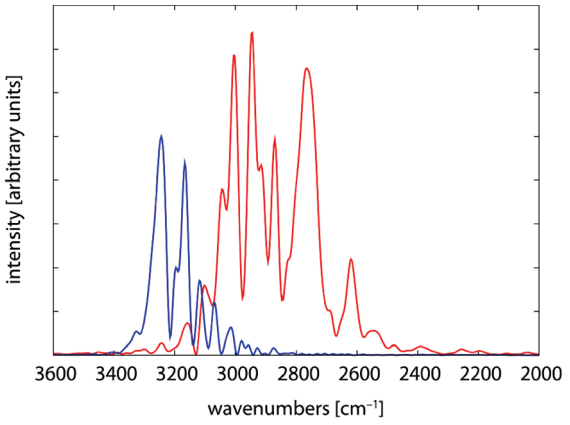

Figure 9. Vibrational power spectra of the selected four N−H bond distances in histamine. The intensities are in arbitrary units. Blue curve corresponds to the ring amino N−H absorption, while the red curve depicts N−H stretching frequencies from all three free−amino hydrogen atoms.

group. However, quantitative predictions of this accuracy are beyond the scope and the accuracy of the present methodology. Hence, we treated the contributions of all N−H groups to the IR spectrum as "equal".

Experimental IR spectrum of protonated histamine in aqueous solution is shown in Figure 4. It exhibits a broad band covering the range from 3600 cm^{-1} to 2300 cm^{-1}. The focal point of the comparison between the calculated and the experimental IR spectrum is the N−H stretching region around 3000 cm^{-1}, since these degrees of freedom are responsible for biological function of histamine. The extracted autocorrelation function of the four N−H bond distances was obtained from the CPMD trajectory. Then, Fourier transformations of the obtained autocorrelation functions were deduced, which have resulted in four IR absorptions corresponding to each N−H stretching vibrations. We grouped the three chain−amino N−H contours into a single curve, whereas the N−H contour related to the ring amino nitrogen is treated separately. The resulting vibrational power spectrum is presented in Figure 9. The calculated IR spectrum compares reasonably well with the experiment, concerning the position of the main bands, but the agreement is far from being perfect. However, it is evident from Figure 9 that calculated spectrum appears as a broad absorption located between 3400 cm^{-1} and 2500 cm^{-1}. Therefore, the obtained absorption shapes are blue-shifted by some 200 cm^{-1} in the lower part and by around 100 cm^{-1} in the upper part of the spectrum. Similar discrepancy was already identified in the literature by some authors.[86,87] The origin of this error is associated with the lack of explicit treatment of the quantum nature of nuclear motion. Imperfections of the BLYP density functional and further technical approximations inherent to the *ab initio* CPMD methodology cannot be disregarded either. Therefore, it is necessary to include nuclear quantum effects in the treatment of the hydrogen atom dynamics to correctly account for the anharmonic effects. Nevertheless, the calculated spectra reveals that all three amino N−H stretching vibrations in the aminoethyl side chain absorb at notably lower frequencies than the ring N−H group does. This is not surprising, since the N−H chemical bond in the charged $-NH_3^+$ group is weaker than that in the ring amino group. Thus, the former group forms a stronger interaction with the surrounding water molecules, as a result and due to more favorable charge−dipole interactions.

Snapshot Anharmonic Frequencies and the NH Stretching Envelope. By solving the vibrational Schrödinger equation for the longitudinal proton motion, we obtained a set of fundamental excitation frequencies that correspond to 0→1 vibrational transitions. These frequencies span a wide range from 3229 cm^{-1} to 2136 cm^{-1} (Figure 10). Such a wide range originates from the very diverse snapshot geometries used to calculate proton potentials of different shapes. This distribution of frequencies determines the shape of the NH stretching band ("NH stretching envelope") of all four N−H chemical bonds present in the histamine monocation due to a coupling of the hydrogen bonds with the fluctuating environment. The NH stretching envelope is used in obtaining a continuous plot by assuming a Gaussian function for each transition as mentioned in the Computational Details. The resulting function resembles a Gaussian-type shape with the maximum absorption in the range between 2820 cm^{-1} and 2730 cm^{-1}. The center of gravity of this function, calculated as the average of all individual transition frequencies, takes the value of 2799 cm^{-1}. It is important to point out that the resulting absorption envelope is in excellent agreement with the experimentally determined vibrational spectra presented in Figure 4, being notably better than the calculated contours using Fourier transformation of the bond distances (Figure 9). This holds for both the position and the shape of the spectral line. These findings lend credence to the approach adopted here, thus providing convincing evidence of the importance of the dynamical aspects of the vibrating hydrogen bonds as well as nuclear quantum effects on the vibrational transitions. For the sake of comparison, we performed intrinsic gas-phase and implicit PCM solvation analysis of the stationary harmonic vibration frequencies for the protonated histamine at the B3LYP/6-311+G(d,p) and (PCM)/B3LYP/6-311+G(d,p) levels of theory, respectively. The resulting transitions in the gas-phase appear grossly blue-shifted as evidenced by the following frequencies: 3638 cm^{-1} for the N−H stretching of the five-membered ring amino group, and 3484 and 3401 cm^{-1} for the asymmetric and symmetric stretching modes of the free-cationic amino group, respectively. The corresponding values in the PCM solution assume 3635, 3500, and 3422 cm^{-1}, in the same order. Two things are interesting and noteworthy. First, inclusion of the implicit PCM model for aqueous solution does not change the corresponding vibrational frequencies much. Second, both sets of values are equally erroneous, not only in that they cannot reproduce experimental

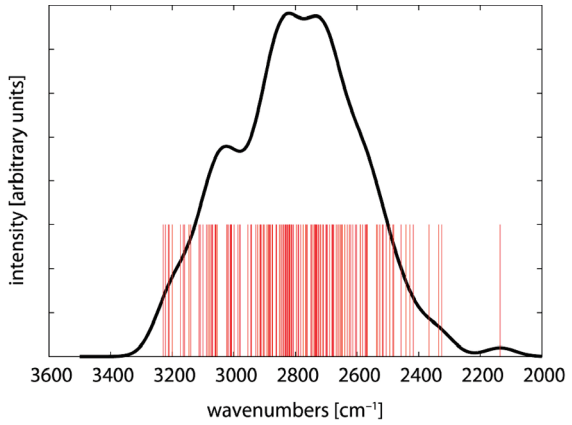

Figure 10. Distribution of anharmonic NH stretching transitions (red vertical lines) obtained from proton potentials extracted from snapshot structures of the CPMD simulation. A continuous representation of this distribution (black curve) is obtained as a superposition of the Gaussian functions (one for each transition) with a half width of 50 cm^{-1}.

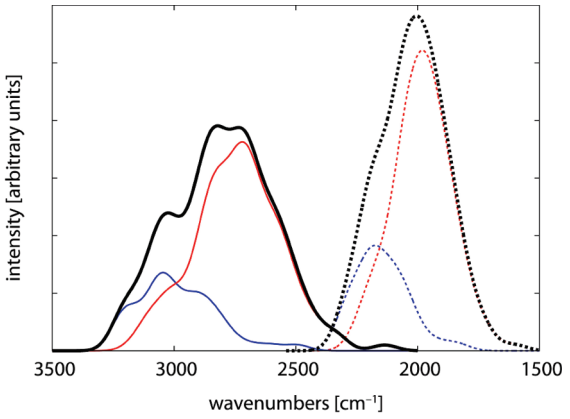

Figure 11. N−H (solid lines) and N−D (dashed lines) stretching envelopes modeled from individual 0→1 vibrational transitions as a superposition of Gaussian functions with a half width of 50 cm^{-1}. Black lines represent cumulative N−H(D) stretching vibrational spectra, consisting of contributions arising from free amino (red lines) and ring amino (blue lines) groups.

spectra, but surprisingly enough, both sets of data are so much shifted to higher frequencies that they even fall outside the shape area of the experimental spectra in that region. Even the application of the appropriate gas-phase frequency scaling factors would not change this picture, since for this kind of the applied computational level of theory the vibrational scaling factors are very close to 1, as recently demonstrated by Johnson[88] and Truhlar[89] and their co-workers. This provides conclusive evidence that discrete solvation models are necessary in the studies of aqueous vibrational spectra.

Our snapshot approach allows us also to consider each of the stretching vibrational modes separately. Therefore, it is capable of distinguishing the signals in the spectrum originating from different N−H bonds, e.g., from the $-NH_3^+$ group or from the ring amino group. If all three stretching motions of the protonated aminoethyl moiety are grouped together, the resulting transitions in the spectra take the form presented in Figure 11. It turns out that the ring amino group absorbs IR light at higher frequencies than the $-NH_3^+$ group. This represents one of the advantages of our computational approach, since it is very difficult to make such distinction by spectroscopic measurements alone.

Deuteration of the solvent molecules, in most instances replacing H_2O with D_2O, represents a very powerful experimental technique to examine and probe the reaction mechanisms in solution.[90] The response to deuteration is also used by experimentalists as a query of the intermolecular hydrogen bonding between solvent molecules and specific hydrophilic sites of a solute. The computational approach expounded here could be used in an analogous way to eliminate ambiguities in the assignment of the spectra. Therefore, it is of some interest to investigate the changes in the vibrational spectra of histamine monocation upon deuteration. An attempt to account for the deuteration effect was also made, employing the same classical trajectory corresponding to the N−H···OH_2 solvation situation of histamine, in conjunction with the matching snapshot potentials. It has been used to obtain the envelope of the N−D stretching band. This was performed by subsequently solving the vibrational Schrödinger equation with the increased reduced mass corresponding to the heavier D nucleus. At first sight it might be expected that the experimentally recorded spectra presented in Figure 4 and the computationally obtained stretching envelope would not be comparable. Namely, the experimental deuterated spectra originate mostly from the N−H···OD_2, and partially from the N−D···OD_2 subsystems, whereas the computational absorption spectra arise from the N−D···OH_2 subsystem. However, the use of the same trajectory for the modeling of both the N−H and N−D bands is legitimate, because thermal averages of classical trajectories, and thus all the snapshot structures and proton potential energy functions, are ensemble averages and, in the framework of classical statistical mechanics, independent of nuclear masses. This assumption is well-established in classical simulations, but it was recently successfully employed in the CPMD studies.[91] Still, this might not always be the case, and certain care must be exerted. Isotopic substitution could lead to varying oscillation amplitudes, which could propagate further to other, non-isotopically substituted degrees of freedom. However, we do not believe that such indirect effect should be large and can conclude that, within the reasonable approximation, our model of the N−H (N−D) vibrational envelopes is insensitive to the isotope composition of the environment. The resulting N−D stretching envelope, presented also in Figure 11, is fairly similar in shape to the corresponding N−H counterpart. However, it is much narrower and is red-shifted by some 750 cm^{-1}. The pattern observed for the N−H vibrations in terms of the position of the contributions arising from $-NH_3^+$ and ring amino group stretching is also maintained in the case of deuterium. In order to estimate the ν(N−H)/ν(N−D) isotope ratio, it is sensible to consider stretching vibrations of the ring amino N−H bond. The corresponding centers of gravity for both NH and ND envelopes of the ring amino groups assume values of 2983 and 2145 cm^{-1}, respectively. It follows that the deduced ν(N−H)/ν(N−D) isotope ratio equals 1.39, which fits into the harmonic approximation. This conclusion has to be taken with some care, however, since the shapes of the matching hydrogen versus deuterium curves in the calculated spectra are not identical over the whole range of wave numbers (Figure 11). This implies that if each snapshot vibrational transition along the spectrum is considered, the isotope ratio could differ from this almost ideal harmonic value. In fact, as can be seen from Figure 11, despite the

dx.doi.org/10.1021/jp111175e |J. Phys. Chem. B 2011, 115, 5999–6010

fact that the isotope ratio averaged over all potentials approaches a nearly harmonic value of $\sqrt{2}$, only a small portion of them have the corresponding NH/ND frequency ratio close to it. Instead, this ratio is very often higher or lower than $\sqrt{2}$ by 0.2, as observed earlier in some very strong hydrogen bonds.[31]

PERSPECTIVES

First-principle MD simulations based on the description of interatomic interactions evaluated from electronic structure calculations as the simulation proceeds have a long and successful record in the study of biomolecular systems, material science, and chemical problems. This holds in particular for the treatment of medium-sized molecules in condensed phase, either in solutions or in crystals. One of the advantages of *ab initio* MD is that it easily permits a close connection with the experimental data, for example with IR, Raman, and NMR spectroscopy.[92,93] The data for solutes obtained from IR spectroscopy, which probe the hydrogen bonding ability of the acidic and basic sites and hydration dynamics, are crucial for the understanding of the role these molecules play in biological processes such as binding to large macromolecules, receptor activation, and transport through membrane and ion channels. The computational methodology presented in this study is very effective for the description of the dynamics of strongly correlated systems such as hydrogen bonds. The idea of the snapshot envelope methods is, however, not new and unknown. Our main contribution originates from the fact that we were among first to implement it within the Car−Parrinello methodology. Generally speaking, this approach was previously used in numerous occasions to study, for example, ion hydration and OH stretching modes.[94,95] It was also applied in the context of molecular simulations based on empirical force fields,[96,97] and in the study of highly anharmonic systems.[71,98−100] Some of us also utilized it to investigate hydrogen bonded systems in the solid state[31,101] and in apolar solvent.[102] An overview of computational methods treating dynamics of hydrogen bonded systems, including isotope effects and spectroscopic properties could be found in several books that recently appeared in the literature.[2,90,103]

In this work we obtained a very good agreement between snapshots calculated and experimentally obtained N−H stretching bands. For deuterated histamine, a less satisfactory agreement was found. The center of the experimental N−D stretching band is located at 2340 cm^{-1}, while the calculated value assumes around 2000 cm^{-1}. More research on various systems is necessary before a general assessment of the accuracy of the applied methodology could be made. A more rigorous way to prepare structures of the snapshots is offered by path-integral molecular dynamics (PIMD) in the framework of the CPMD. In this way the Ubbelohde effect,[104] stating that deuteration of hydrogen bonded systems changes the effective proton donor−proton distance as well as the proton donor−proton acceptor distance, would also be included in the simulation. We believe that quantization of additional degrees of freedom, such as, for example, O···N stretching and N−H(D) bending motions, should improve overall agreement with the experiment. The extension of this methodology to two or more dimensions is conceptually straightforward. However, it is worth emphasizing that both path−integral simulation and quantization of additional degrees of freedom would be associated with a huge increase in the computing time, which would require enormously large computer resources.

The presented approach is intended to be a relatively inexpensive way of introducing *a posteriori* quantum corrections to any classical MD trajectory. Thus, it could be useful, for example, in investigations of the nuclear tunneling in enzyme reactive centers either by CPMD simulations, some classical force-field dynamics, or by one of the established QM/MM techniques.[105−107] Recent studies clearly demonstrated the relevance of hydrogen bonding in the receptor activation.[108] It remains a major challenge to study receptor triggering with molecular simulation and to provide *in silico* differentiation between agonist and antagonist activity. Our approach is very general in its nature and particularly tuned to meet the needs of vibrational spectroscopy. With this detailed account of an application to a single molecule, we hope to have presented convincing evidence of the potential this approach has in the large field of condensed-phase *ab initio* MD-based computational spectroscopy.

CONCLUDING REMARKS

In a combined computational and experimental FTIR spectroscopic study, we investigated the nature of hydration of a histamine monocation that corresponds to the aminoethyl protonated state of histamine at physiological conditions. CPMD simulation of 10 ps was performed for the histamine monocation and Cl^- anion as a counterion immersed in a box of water molecules. The nature of hydration is experimentally reflected in the N−H stretching frequencies. We calculated the contour of the N−H stretching band (i) by utilizing Fourier transformation of the autocorrelation function of selected N−H bond distances, and (ii) by performing an *a posteriori* quantization of the N−H stretching motion to snapshot structures obtained after CPMD simulation. Very good agreement between experimental and calculated spectra was found for the latter approach in terms of the shape and the position of the N−H stretching bands. It is demonstrated that amino protons of the protonated aminoethyl side chain are involved in stronger hydrogen bonding with the surrounding water molecules than their ring N−H counterparts. The corresponding calculated stretching frequencies of the chain-amino N−H bonds versus the ring N−H ones peak at 2720 and 3045 cm^{-1}, respectively. This conclusion was further corroborated by (a) inspecting the relevant N(histamine)···O(water) distances during CPMD run, which are on average larger for ring amino group; (b) by considering the radial distribution functions between both nitrogen sites and the surrounding water molecules, which show a higher first hydration peak for the chain-amino group; and (c) by a separate gas-phase and implicit PCM solvent analysis of the microsolvation effects on the histamine cation, revealing lower enthalpy of interaction for the ring amino moiety. Experimentally, one cannot distinguish between the two N−H stretching bands. Instead, the center of the cumulative band was found at 2950 cm^{-1}. The effects of deuteration were also considered. It is found that the isotope ratio ν(N−H)/ν(N−D) assumes a value of 1.39. To epitomize, the utilized methodology is of general applicability for strongly anharmonic motions in the condensed and gas phases in much larger systems and represents a powerful tool for computational support to vibrational spectroscopy.

ASSOCIATED CONTENT

Supporting Information. Raw experimental FTIR ATR vibrational spectra of histamine monocation in H_2O and D_2O

recorded at pH = 7.4, and details on the selection of the appropriate plane-wave kinetic energy cutoff value for CPMD simulation. This material is available free of charge via the Internet at http://pubs.acs.org.

AUTHOR INFORMATION

Corresponding Author

*Telephone: +386−1−4760453. Fax: +386−1−4760300. E-mail: robert.vianello@irb.hr.

Notes

[||]Deceased.

ACKNOWLEDGMENT

It is with great sadness that we acknowledge the unexpected death of our colleague, mentor, and friend, Professor Zvonimir B. Maksić on March 27, 2011. He will be mourned by the scientific community at large. We thank the Slovenian Research Agency and the Croatian Ministry of Science, Education, and Sport for the financial support in the framework of the bilateral scientific cooperation agreement. This work has been carried out in the framework of the program groups with program codes P1-0012 and P1-0010 and within the corresponding research project contract Nos. J1-2014 and J1-2252. R.V. gratefully acknowledges the European Commission for an individual FP7 Marie Curie Intra European Fellowship for the Career Development; Contract Number PIEF-GA-2009-255038 and is thankful for some financial support from the National Foundation for Science, Higher Education, and Technological Development of the Republic of Croatia.

REFERENCES

(1) Buckingham, A. D.; Del Bene, J. E.; McDowell, S. A. C. *Chem. Phys. Lett.* **2008**, *463*, 1.
(2) *Hydrogen Transfer Reactions*; Hynes, J. T., Klinman, J. P., Limbach, H.-H., Schowen, R. L., Eds.; Wiley-VCH: Weinheim, Germany, 2006.
(3) Maréchal, Y. *The Hydrogen Bond and the Water Molecule*; Elsevier: Amsterdam, 2007.
(4) *Proton Transfer in Hydrogen-Bonded System*; Bountis, D., Ed.; Plenum: New York, 1992.
(5) Busca, G. *Chem. Rev.* **2007**, *107*, 5366.
(6) Busca, G. *Chem. Rev.* **2010**, *110*, 2217.
(7) *Electron and Proton Transfer in Chemistry and Biology*; Müller, A., Ratajczak, H., Junge, W., Diemann, E., Eds.; Elsevier: Amsterdam, 1992.
(8) Dror, R. O.; Arlow, D. H.; Borhani, D. W.; Jensen, M. Ø.; Piana, S.; Shaw, D. E. *Proc. Natl. Acad. Sci. U.S.A.* **2009**, *106*, 4689.
(9) Dobson, P. D.; Kell, D. B. *Nature* **2008**, *7*, 205.
(10) Bucher, D.; Rothlisberger, U. *J. Gen. Physiol.* **2010**, *135*, 549.
(11) Dror, R. O.; Jensen, M. Ø.; Borhani, D. W.; Shaw, D. E. *J. Gen. Physiol.* **2010**, *135*, 555.
(12) Silva, J. R.; Rudy, Y. *J. Gen. Physiol.* **2010**, *135*, 575.
(13) Barger, G.; Dale, H. H. *J. Physiol. (London)* **1910**, *41*, 19.
(14) Pegg, A. E. *Cancer Res.* **1988**, *759*, 48.
(15) Hill, S. J.; Ganellin, C. R.; Timmerman, H.; Schwartz, J. C.; Shankley, N. P.; Young, J. M.; Schunack, W.; Levi, R.; Haas, H. L. *Pharmacol. Rev.* **1997**, *49*, 253.
(16) Schneider, E.; Rolli-Derkinderen, M.; Arock, M.; Dy, M. *Trends Immunol.* **2002**, *23*, 255.
(17) Passani, M. B.; Giannoni, P.; Bucherelli, C.; Baldi, E.; Blandina, P. *Biochem. Pharmacol.* **2007**, *73*, 1113.
(18) Tashiro, M.; Yanai, K. *Brain Nerve* **2007**, *59*, 221.
(19) Sheppard, N. In *Hydrogen Bonding*; Hadži, D., Thomson, H., Eds.; Pergamon Press: London, 1959.
(20) Bratos, S.; Leicknam, J.-Cl.; Gallot, G.; Ratajczak, H. In *Ultrafast Hydrogen Bonding and Proton Transfer Processes in the Condensed Phase*; Elsaesser, T., Bakker, H. J., Eds.; Kluwer Academic Publishers: Dordrecht, The Netherlands, 2002 (and references therein).
(21) Cho, M. *Chem. Rev.* **2008**, *108*, 1331.
(22) Kim, Y. S.; Hochstrasser, R. M. *J. Phys. Chem. B* **2009**, *113*, 8231.
(23) Tew, D. P.; Klopper, W.; Heckert, M.; Gauss, J. *J. Phys. Chem. A* **2007**, *111*, 11242.
(24) Martin, J. M.; Lee, T. J.; Taylor, P. R.; Francois, J.-P. *J. Chem. Phys.* **1995**, *103*, 2589.
(25) Burcl, R.; Handy, N. C.; Carter, S. *Spectrochim. Acta, Part A* **2003**, *59*, 1881.
(26) Boese, A. D.; Martin, J. *J. Phys. Chem. A* **2004**, *108*, 3085.
(27) Barone, V. *J. Chem. Phys.* **2005**, *122*, 014108.
(28) Puzzarini, C.; Barone, V. *Phys. Chem. Chem. Phys.* **2008**, *10* 6991.
(29) Bowman, J. M. *Acc. Chem. Res.* **1986**, *19*, 202.
(30) Car, R.; Parrinello, M. *Phys. Rev. Lett.* **1985**, *55*, 2471.
(31) Pirc, G.; Stare, J.; Mavri, J. *J. Chem. Phys.* **2010**, *132*, 224506.
(32) Wong, K. F.; Sonnenberg, J. L.; Paesani, F.; Yamamoto, T.; Vaníček, J.; Zhang, W.; Schlegel, H. B.; Case, D. A.; Cheatham, T. E., III; Miller, W. H.; Voth, G. A. *J. Chem. Theory Comput.* **2010**, *6*, 2566.
(33) Swalina, C.; Wang, Q.; Chakraborty, A.; Hammes-Schiffer, S. *J. Phys. Chem. A* **2007**, *111*, 2206.
(34) Webb, S. P.; Iordanov, T.; Hammes-Schiffer, S. *J. Chem. Phys.* **2002**, *117*, 4106.
(35) Demšar, K.; Stare, J.; Mavri, J. *J. Mol. Struct.* **2007**, *844−845*, 215.
(36) Stare, J.; Mavri, J. *Comput. Phys. Commun.* **2002**, *143*, 222–240.
(37) Stare, J.; Balint-Kurti, G. G. *J. Phys. Chem. A* **2003**, *107*, 7204.
(38) Mavri, J.; Grdadolnik, J. *J. Phys. Chem. A* **2001**, *105*, 2039.
(39) Došlić, N.; Kühn, O. *Z. Phys. Chem.* **2003**, *217*, 1507.
(40) Matanović, I.; Došlić, N. *J. Phys. Chem. A* **2005**, *109*, 4185.
(41) Bowman, J. M. *Acc. Chem. Res.* **1986**, *19*, 202.
(42) Rauhut, G.; Knizia, G.; Werner, H. J. *J. Chem. Phys.* **2009**, *130*, 054105.
(43) Relph, R. A.; Guasco, T. L.; Elliott, B. M.; Kamrath, M. Z.; McCoy, A. B.; Steele, R. P.; Schofield, D. P.; Jordan, K. D.; Viggiano, A. A.; Ferguson, E. E.; Johnson, M. A. *Science* **2010**, *327*, 308.
(44) Wójcik, M. J.; Kwiendacz, J.; Boczar, M.; Boda, Ł.; Ozaki, Y. *Chem. Phys.* **2010**, *372*, 72.
(45) Paiva, T. B.; Tominaga, M.; Paiva, A. C. M. *J. Med. Chem.* **1970**, *1*, 689.
(46) Perdan-Pirkmajer, K.; Mavri, J.; Kržan, M. *J. Mol. Model.* **2010**, *16*, 1151.
(47) Ramírez, F. J.; Tuñón, I.; Collado, J. A.; Silla, E. *J. Am. Chem. Soc.* **2003**, *125*, 2328.
(48) Weisntein, H.; Chou, E.; Johnson, C. L.; Kang, S.; Green, J. P. *Mol. Pharmacol.* **1976**, *12*, 738.
(49) Collado, J. A.; Tuñón, I.; Silla, E.; Ramírez, F. J. *J. Phys. Chem. A* **2000**, *104*, 2120.
(50) Bellocq, A. M.; Garrigou-Lagrange, C. *J. Chim. Phys. Physico-chim. Biol.* **1970**, *64*, 1544.
(51) Collado, J. A.; Ramírez, F. J. *J. Raman Spectrosc.* **1999**, *30*, 391.
(52) Collado, J. A.; Ramírez, F. J. *J. Raman Spectrosc.* **2000**, *31*, 925.
(53) Drozdzewski, P.; Kordon, E. *Spectrochim. Acta* **2000**, *56*, 1299.
(54) Drozdzewski, P.; Kordon, E. *Spectrochim. Acta* **2000**, *56*, 2459.
(55) Drozdzewski, P.; Kordon, E. *Vib. Spectrosc.* **2000**, *24*, 243–248.
(56) Ganellin, C. R. *J. Pharm. Pharmacol.* **1973**, *25*, 787.
(57) Worth, G. A.; Richards, W. G. *J. Am. Chem. Soc.* **1994**, *116*, 139.
(58) Arteca, G. A.; Hernández-Laguna, A.; Rández, J. J.; Smeyers, Y. G.; Mezey, P. *J. Comput. Chem.* **1991**, *12*, 705.
(59) Xerri, B.; Flament, J.-P.; Petitjean, H.; Berthomieu, C.; Berthomieu, D. *J. Phys. Chem. B* **2009**, *113*, 15119.
(60) Bertie, J. E.; Lan, Z. *J. Chem. Phys.* **1996**, *105*, 8502.
(61) Grdadolnik, J.; Maréchal, Y. *J. Mol. Struct.* **2002**, *615*, 177.
(62) Grobelnik, B.; Grdadolnik, J. *Acta Chim. Sloven* **2008**, *55*, 978.
(63) CPMD V3.13, Copyright IBM Corp 1990−2008, Copyright MPI fuer Festkoerperforschung Stuttgart 1997−2001.

(64) (a) Becke, A. *Phys. Rev. A* **1988**, *38*, 3098. (b) Lee, C.; Yang, W.; Parr, R. *Phys. Rev. B* **1988**, *37*, 785.
(65) Troullier, N.; Martins, J. L. *Phys. Rev. B* **1991**, *43*, 1993.
(66) Nosé, S. *J. Chem. Phys.* **1984**, *81*, 511.
(67) Nosé, S. *Mol. Phys.* **1984**, *52*, 255.
(68) Hoover, W. G. *Phys. Rev. A* **1985**, *31*, 1695.
(69) VandeVondele, J.; Krack, M.; Mohamed, F.; Parrinello, M.; Chassaing, T.; Hutter, J. *Comput. Phys. Commun.* **2005**, *167*, 103.
(70) Ojamae, L.; Hermansson, K.; Probst, M. *Chem. Phys. Lett.* **1992**, *191*, 500.
(71) Ojamae, L.; Tegenfeldt, J.; Lindgren, J.; Hermansson, K. *Chem. Phys. Lett.* **1992**, *195*, 97.
(72) Rey, R.; Moller, K. B.; Hynes, J. T. *J. Phys. Chem. A* **2002**, *106* 11993.
(73) Moller, K. B.; Rey, R.; Hynes, J. T. *J. Phys. Chem. A* **2004**, *108* 1275.
(74) Corcelli, S. A.; Lawrence, C. P.; Skinner, J. L. *J. Chem. Phys.* **2004**, *120*, 8107.
(75) Balint-Kurti, G. G.; Dixon, R. N.; Marston, C. C. *Int. Rev. Phys. Chem.* **1992**, *11*, 317.
(76) MacKerell, A. D., Jr.; Bashford, D.; Bellott, M.; Dunbrack, R. L., Jr.; Evanseck, J. D.; Field, M. J.; Fischer, S.; Gao, J.; Guo, H.; Ha, S.; Joseph-McCarthy, D.; Kuchnir, L.; Kuczera, K.; Lau, F. T. K.; Mattos, C.; Michnick, S.; Ngo, T.; Nguyen, D. T.; Prodhom, B.; Reiher, W. E., III; Roux, B.; Schlenkrich, M.; Smith, J. C.; Stote, R.; Straub, J.; Watanabe, M.; Wiórkiewicz-Kuczera, J.; Yin, D.; Karplus, M. *J. Phys. Chem. B* **1998**, *102*, 3586.
(77) Brooks, B. R.; Bruccoleri, R. E.; Olafson, B. D.; States, D. J.; Swaminathan, S.; Karplus, M. *J. Comput. Chem.* **1983**, *4*, 187.
(78) Essmann, U.; Perera, L.; Berkowitz, M. L.; Darden, T.; Lee, H.; Pedersen, L. G. *J. Chem. Phys.* **1995**, *103*, 8577.
(79) Humphrey, W.; Dalke, A.; Schulten, K. *J. Mol. Graphics* **1996**, *14*, 33.
(80) Frisch, M. J.; Trucks, G. W.; Schlegel, H. B.; Scuseria, G. E.; Robb, M. A.; Cheeseman, J. R.; Scalmani, G.; Barone, V.; Mennucci, B.; Petersson, G. A.; Nakatsuji, H.; Caricato, M.; Li, X.; Hratchian, H. P.; Izmaylov, A. F.; Bloino, J.; Zheng, G.; Sonnenberg, J. L.; Hada, M.; Ehara, M.; Toyota, K.; Fukuda, R.; Hasegawa, J.; Ishida, M.; Nakajima, T.; Honda, Y.; Kitao, O.; Nakai, H.; Vreven, T.; Montgomery, Jr., J. A.; Peralta, J. E.; Ogliaro, F.; Bearpark, M.; Heyd, J. J.; Brothers, E.; Kudin, K. N.; Staroverov, V. N.; Kobayashi, R.; Normand, J.; Raghavachari, K.; Rendell, A.; Burant, J. C.; Iyengar, S. S.; Tomasi, J.; Cossi, M.; Rega, N.; Millam, N. J.; Klene, M.; Knox, J. E.; Cross, J. B.; Bakken, V.; Adamo, C.; Jaramillo, J.; Gomperts, R.; Stratmann, R. E.; Yazyev, O.; Austin, A. J.; Cammi, R.; Pomelli, C.; Ochterski, J. W.; Martin, R. L.; Morokuma, K.; Zakrzewski, V. G.; Voth, G. A.; Salvador, P.; Dannenberg, J. J.; Dapprich, S.; Daniels, A. D.; Farkas, Ö.; Foresman, J. B.; Ortiz, J. V.; Cioslowski, J.; Fox, D. J. *Gaussian 09*, revision A.1; Gaussian, Inc.: Wallingford, CT, 2009.
(81) Tomasi, J.; Mennucci, B.; Cammi, R. *Chem. Rev.* **2005**, *105*, 2999.
(82) Silvestrelli, P. L.; Bernasconi, M.; Parrinello, M. *Chem. Phys. Lett.* **1997**, *277*, 478.
(83) Bernasconi, M.; Silvestrelli, P. L.; Parinello, M. *Phys. Rev. Lett.* **1998**, *81*, 1235.
(84) Putrino, A.; Parrinello, M. *Phys. Rev. Lett.* **2002**, *88*, 176401.
(85) Wannier, G. H. *Phys. Rev.* **1937**, *52*, 191.
(86) Gaigeot, M.-P.; Sprik, M. *J. Phys. Chem. A* **2003**, *107*, 10344.
(87) Gaigeot, M.-P. *J. Phys. Chem. A* **2008**, *112*, 13507.
(88) Johnson, R. D., III; Irikura, K. K.; Kacker, R. N.; Kessel, R. *J. Chem. Theory Comput.* **2010**, *6*, 2822.
(89) Alecu, I. M.; Zheng, J.; Zhao, Y.; Truhlar, D. G. *J. Chem. Theory Comput.* **2010**, *6*, 2872.
(90) *Isotope Effects in Chemistry and Biology*; Kohen, A., Limbach, H.-H., Eds.; CRC Press: New York, 2005.
(91) Salanne, M.; Simon, C.; Madden, P. A. *Phys. Chem. Chem. Phys.* **2011**, *13*, 6305.
(92) Marx, D.; Hutter, J. *Ab Initio Molecular Dynamics: Basic Theory and Advanced Methods*; Cambridge University Press: Cambridge, U.K., 2009.
(93) Perrin, C. A. *Acc. Chem. Res.* **2010**, *43*, 1550.
(94) Pejov, L.; Spangberg, D.; Hermansson, L. *J. Phys. Chem. A* **2005**, *109*, 5144.
(95) Ojamäe, L.; Tegenfeldt, J.; Lindgren, J.; Hermansson, K. *Chem. Phys. Lett.* **1992**, *195*, 97.
(96) Li, S.; Schmidt, J. R.; Piryatinski, A.; Lawrence, C. P.; Skinner, J. L. *J. Phys. Chem. B* **2006**, *110*, 18933.
(97) Bakker, H. J.; Skinner, J. L. *Chem. Rev.* **2010**, *110*, 1498.
(98) Yan, Y.; Kuhn, O. *Phys. Chem. Chem. Phys.* **2010**, *12*, 15695.
(99) Yan, Y.; Petković, M.; Krishnan, G. M.; Kuhn, O. *J. Mol. Struct.* **2010**, *972*, 68.
(100) Cyrański, M. K.; Jezierska, A.; Klimentowska, P.; Panek, J. J.; Zukowska, G. Z.; Sporzyński, A. *J. Chem. Phys.* **2008**, *128*, 124512.
(101) Stare, J.; Panek, J.; Eckert, J.; Grdadolnik, J.; Mavri, J.; Hadži, D. *J. Phys. Chem. A* **2008**, *112*, 1576.
(102) Jezierska, A.; Panek, J.; Borštnik, U.; Mavri, J.; Janežič, D. *J. Phys. Chem. B* **2007**, *111*, 5243.
(103) *Quantum Tunneling in Enzyme-Catalysed Reactions*; Alleman, R. K., Scrutton, N. S., Eds.; RSC Publishing: Cambridge, 2009.
(104) Ubbelohde, A. R.; Gallagher, K. J. *Acta Crystallogr.* **1955**, *8*, 71.
(105) Rosta, E.; Klähn, M.; Warshel, A. *J. Phys. Chem. B* **2006**, *110*, 2934.
(106) Carloni, P.; Rothlisberger, U.; Parrinello, M. *Acc. Chem. Res.* **2002**, *35*, 455.
(107) Warshel, A. *Computer Modeling of Chemical Reactions in Enzymes and Solutions*; John Wiley & Sons: New York, 1997.
(108) Nygaard, R.; Frimurer, T. M.; Holst, B.; Rosenkilde, M. M.; Schwartz, T. W. *Trends Pharmacol. Sci.* **2009**, *30*, 249.